Materials for Renewable and Sustainable Energy (2025) 14:13
https://doi.org/10.1007/s40243-024-00291-6

ORIGINAL PAPER

Triple-junction tandem solar cells: structural and spectral optimization for improved current matching and efficiency

Hugo Rolando Sánchez Quispe[1] · Prakash Kanjariya[2] · Suhas Ballal[3] · Anita Devi[4] · Girish Chandra Sharma[5] · Radhwan Abdul Kareem[6] · K. Satyam Naidu[7] · Marwea Al-hedrewy[8,9] · Ashish Kumar[10] · Asaithambi Perumal[11]

Received: 11 November 2024 / Accepted: 18 December 2024

Abstract
In this work, a triple-junction tandem solar cell (TSC) has been designed in order to increase the photovoltaic (PV) performance through utilizing maximum light photons. To create three junctions in this work three subcells have been designed and optimized at its best PV performance. The optimization of all the three subcells have been done through the various variations in the absorber layer like thickness and bulk defect density (BDD). It has been seen that best PV parameters in the top middle and bottom cell are maximum at high thickness and low BDD. For the designing of triple junction tandem configuration, two filtered spectrums (FS1 and FS2) have been calculated for the proper current matching in the three subcells. The optimized triple-junction TSC demonstrates significantly enhanced PV parameters, including high open-circuit voltage (V_{OC}- 2.750), short-circuit current density (J_{SC}- 16.45 mA/cm^2), fill factor (FF- 83.40%), and power conversion efficiency (PCE- 37.74%). The strategy of using filtered spectrums and exact design optimization provides a potential road to the next generation of high-efficiency tandem solar cells, furthering the field of renewable energy solutions.

Keywords Photovoltaic · SCAPS-1d · Tandem solar cell · Current matching · Filtered spectrum · Optimization

Introduction

In the modern era renewable energy resources are very dominant in the energy conversion [1]. Among all the renewable energy resources, solar energy is untapped energy which is utilized for the electricity conversion. Photovoltaic (PV) performance of single junction solar cells are limited according to the S-Q limit [2, 3]. To break that limit multi-junction solar cells are designed by various researchers till date [4–6]. As per literatures, various double and triple junction tandem solar cells have been designed. 3JTSC provides several advancement in PV technology by breaking the efficiency limit which is predicted by S-Q [7, 8]. In typical single-junction cells, a significant amount of sunlight is either

✉ Asaithambi Perumal
asaithambi.perumal@ju.edu.et;
drasaithambi2014@gmail.com

1 Escuela Superior Politécnica de Chimborazo (ESPOCH), Sede Orellana, El Coca 220202, Ecuador

2 Department of Physics, Faculty of Science, Marwadi University Research Center, Marwadi University, Rajkot, Gujarat 360003, India

3 Department of Chemistry and Biochemistry, School of Sciences, JAIN (Deemed to be University), Bangalore, Karnataka, India

4 Department of Chemistry Chandigarh Engineering College, Chandigarh Group of Colleges Jhanjeri, Mohali, Punjab 140307, India

5 Department of Applied Sciences-Chemistry, NIMS Institute of Engineering & Technology, NIMS University Rajasthan, Jaipur, India

6 Ahl Al Bayt University, Kerbala, Iraq

7 Department of Chemistry, Raghu Engineering College, Visakhapatnam, Andhra Pradesh 531162, India

8 College of Technical Engineering, The Islamic University, Najaf, Iraq

9 College of Technical Engineering, The Islamic University of Al Diwaniyah, Al Diwaniyah, Iraq

10 Division of Research and Development, Lovely Professional University, Phagwara, India

11 Faculty of Civil and Environmental Engineering, Jimma Institute of Technology, Jimma University, Po Box - 378, Jimma, Ethiopia

Published online: 21 January 2025

wasting due to thermalisation or goes not absorbed through the cell [9, 10]. 3JTSC achieve higher power conversion efficiency (PCE), as each subcell absorbs a specific range of wavelengths, minimizing energy loss by stacking three cells with progressively narrower bandgaps [11].

The design of these multi-junction cells often incorporates perovskite materials due to their tunable bandgaps, high absorption, and relatively low-cost fabrication [9]. To design the 3JTSC, three subcells have been utilized, top, middle and bottom subcells according to its bandgaps. Wide bandgap materials whose bandgap (1.5-2 eV) are utilized for the designing of top cell whereas bottom and middle have lower bandgap ranges [12, 13]. This architecture is designed as top cell is illuminated by 1.5AMG spectrum of intensity 1000 W/m^2 and middle is illuminated under filtered spectrum coming from top cell. However bottom cell is illuminated through the filtered spectrum passing from top and middle layers. The Shockley-Queisser (S-Q) limit, which defines the theoretical maximum efficiency of a single-junction solar cell under standard illumination conditions, is a critical benchmark in the field of photovoltaic research. In the manuscript, we have referenced the S-Q limit to contextualize the potential performance of single-junction cells. However, to surpass this limit, the use of tandem cells, such as triple-junction solar cells, becomes essential. Triple-junction cells are designed to capture a broader range of the solar spectrum by utilizing multiple absorber layers with different bandgaps. This configuration enables the cells to exceed the S-Q limit for single-junction devices, as each subcell absorbs a distinct portion of the spectrum more efficiently. The use of triple-junction cells is therefore justified as a strategy to achieve higher power conversion efficiencies beyond the theoretical limits of single-junction cells.

Recently, lead-free perovskites are also utilized, which supports in the reduction of toxicity in the environment, present in the conventional perovskite based cells [14, 15]. In the place of conventional PVK, researchers are shifted their research trend towards the leadfree based single junction subcells for the designing of the tandem solar cells [16]. The evolution of multi-junction solar cells began with dual-junction devices, particularly employing III-V semiconductors such as gallium arsenide (GaAs) and indium gallium phosphide (InGaP), which achieved excellent efficiencies but had limits in scalability and cost [17, 18]. With the advent of PVK materials, which have adjustable bandgaps and outstanding absorption optical properties, research into tandem structures has advanced significantly. According to studies conducted by et al. (2018) and Yang et al. (2020), perovskite-based tandem cells can achieve efficiencies of more than 30% under ideal conditions, making them viable replacements to conventional silicon-based PV modules [19]. 3JTSCs usually employ a combination of top, middle, and low-bandgap materials-based bottom cells to improve efficiency through effective spectrum splitting [20]. In particular, recent work by NREL and Oxford PV highlights how wide-bandgap perovskites (e.g., with a bandgap of around 1.6–1.8 eV) serve as efficient top absorbers, followed by a low-bandgap material near 0.9 eV, such as silicon or novel compounds like germanium telluride (GeTe) [21]. The Transfer Matrix Method (TRM) has also been widely adopted to precisely model the absorption and light reflection within these multi-layered cells, as it considers interference, reflection, and refraction more effectively than traditional models [22]. Environmental concerns have prompted research into lead-free perovskite materials, such as $CsSn_{0.5}Ge_{0.5}I_3$, which offer reduced toxicity while maintaining a suitable bandgap for tandem applications. Studies by various researchers and shown that lead-free materials can still deliver competitive efficiencies, though stability under environmental stressors remains an area of active investigation [23]. Furthermore, current matching, which plays an essential role for optimising tandem cell performance, has been extensively investigated, with findings indicating that fine-tuning the thickness of each subcell's absorber layer and optimising electron and hole transport layers are required to achieve balanced photocurrents across each junction. Machine learning techniques have recently become integral in PV research, as demonstrated in work [11, 24]. Researchers are expediting the design process by using machine learning models to optimise layer thickness, material combinations, and current matching, allowing for a more comprehensive investigation of material choices in tandem solar cells. The combination of perovskite materials, machine learning optimisation, and powerful spectral management technologies highlights the advancements in triple-junction tandem solar cells. These research, taken together, establish the framework for developing next-generation PV technologies that are both highly efficient and environmentally sustainable, making them attractive contenders for the future of solar energy. This study specifically addresses the assumptions made in the SCAPS-1D simulations, including the use of idealized material properties, the neglect of certain optical losses, and the simplified treatment of charge transport mechanisms. The challenges in translating the simulated results to real-world applications are also acknowledged, such as the difficulty in achieving precise current matching in the tandem configuration, potential material degradation under operational conditions, and the scalability of fabrication processes. By highlighting these limitations, the study provides a balanced perspective on both the potential and the challenges associated with the proposed design.

This work has been divided into three portions. Section 2 describes the structure of each subcell and the methodology

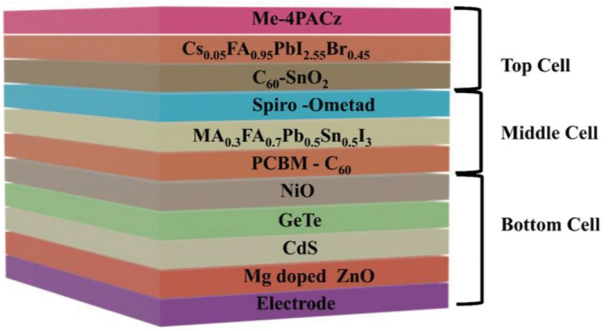

Fig. 1 Cell structure of the single-junction, middle, and bottom cells in a tandem solar cell configuration

utilised in the investigation. Section 3 gives the complete results, which include all areas of the analysis. Finally, Sect. 4 summarises the study's findings.

Device simulation and methodology

The designing of this 3JTSC using SCAPS-1D begins with the proper selection of materials and layers for each subcell. The top cell uses Me4PACz as the hole transport layer (HTL), a perovskite absorber with a 1.62 eV bandgap, and C_{60}-SnO_2 as the electron transport layer (ETL). The middle cell consists of Spiro-OMeTAD as the HTL, a 1.22 eV perovskite absorber, and PCBM-C_{60} as the ETL [7]. In the end, the bottom cell comprises NiO as the HTL, GeTe with a bandgap of 0.88 eV as the absorption layer, and CdS followed by Mg-doped ZnO as the ETL for improved electron extraction. Each layer is engineered for efficient light absorption and charge transmission across the structure, maximising the overall PCE [12]. The complete top, middle and bottom cell structure has been shown in the Fig. 1. All the electrical properties for all the layers have been taken from the published work [7, 12, 25–27] (See Tables 1 and 2).

The Standard Absorption Formula (SAF) is employed to determine the filtered spectrum that reaches each subcell, resulting in the fraction of light transmitted through each layer and absorbed in following cells. This method ensures spectrum overlap between the cells, hence improving current matching, which is critical for high-efficiency tandem devices. Band alignment and interface optimisation are critical in the design process, with a focus on reducing energy barriers and increasing charge extraction at the HTL and ETL interfaces. The interfaces between Me4PACz, perovskite, and C_{60}-SnO_2 in the top cell, Spiro-OMeTAD, perovskite, and PCBM-C_{60} in the middle cell, and NiO, GeTe, CdS, and Mg-doped ZnO in the bottom cell have been optimised to minimise recombination losses and maintain uninterrupted charge movement.

To maximise efficiency, the thickness of each absorber layer is iteratively optimised using SCAPS-1D simulations. The top cell perovskite layer is commonly set to be between 200 and 500 nm, the middle cell perovskite layer between

Table 1 Properties of all materials utilized in the designing of 3 J PVK/PVK/GeTe -based tandem solar cell [7, 12, 25–31]

Properties	Different layers of 3 J perovskite-based tandem solar cell							
	TPAL	MPAL	BPAL	SnO_2	C_{60}	Spiro-OMeTAD	ITO	Me4PACz
Bandgap (eV)	1.60	1.20	0.80	3.60	1.70	3.00	1.16	3.30
Electron affinity (eV)	4.20	4.00	4.8	4.00	3.90	2.45	4.10	2.80
Dielectric Constant	6.5	6.5	36	10	9	3	8.2	10
CB effective density ($/cm^3$)	1×10^{18}	1×10^{18}	1×10^{18}	1×10^{19}	1×10^{19}	1×10^{18}	1×10^{17}	2.5×10^{20}
VB effective density ($/cm^3$)	1×10^{19}	1×10^{19}	1×10^{19}	1×10^{19}	1×10^{19}	1×10^{19}	1×10^{18}	2.5×10^{20}
Electron mobility (cm^2/Vs)	1.6×10^{-1}	1.6×10^{-1}	1.6×10^{-1}	5×10^{1}	5×10^{1}	2×10^{2}	16	6×10^{0}
Hole mobility (cm^2/Vs)	1.6×10^{-1}	1.6×10^{-1}	1.6×10^{-1}	5×10^{1}	5×10^{1}	8×10^{1}	16	2.4×10^{1}
N_D ($/cm^3$)	1×10^{15}	1×10^{15}	1×10^{10}	1×10^{20}	1×10^{18}	-	1×10^{18}	-
N_A ($/cm^3$)	1×10^{15}	1×10^{15}	1×10^{10}	-	-	1×10^{18}	1×10^{18}	1×10^{18}

TPAL- $Cs_{0.05}FA_{0.95}PbI_{2.55}Br_{0.45}$, MPAL-, BPAL- GeTe

Table 2 Comparison of PV parameters obtained in this work with other experimental studies

S. no.	3-junction TSC	V_{OC}	J_{SC}	FF	PCE	Reference
1	PVK/PVK/Si TSC	2.83	11.5	82.08	26.71	[36]
2	PVK/PVK/Si TSC	2.80	8.8	81.10	20.10	[37]
3	All PVK TSC	3.76	10.7	69.00	26.24	[7]
4	PVK/PVK/GeTe TSC	2.70	16.45	83.40	37.74	This work

200 and 600 nm, and the bottom cell's GeTe layer between 500 and 1000 nm. The EQE curves for the top, middle, and bottom cells are displayed in Fig. 2. This iterative method tries to balance photocurrent generation across each subcell, resulting in effective current matching across the structure. Furthermore, bulk and interface defect levels are carefully selected to represent realistic conditions and minimise recombination losses, particularly at HTL/ETL interfaces, where defects can dramatically impair cell performance [32, 33].

Results and discussion

The result section has classified into two sub parts. First subsection 3.1 explains the designing and optimization of the top, middle and bottom subcells. Second subsection describes the designing and methodology of the three junction tandem solar cells.

Optimization of top, middle and bottom subcells

To optimize the tandem solar cell structure, the combined effects of thickness and bulk defect density (BDD) on the photovoltaic (PV) performance of the top, middle, and bottom subcells have been investigated. The simulated design parameters, such as absorber layer thickness and defect density, were selected to optimize the performance of the tandem solar cells within the theoretical framework. However, translating these parameters into practical fabrication presents certain challenges. For instance, achieving the optimal absorber layer thickness in real-world devices requires precise deposition techniques, such as molecular beam epitaxy or metal-organic chemical vapor deposition, which can be challenging for multi-junction structures due to the need for fine control over layer uniformity and material quality. Similarly, minimizing bulk defect density (BDD) is critical for maintaining high device efficiency, but this requires advanced material synthesis and high-purity semiconductor fabrication processes. Defect mitigation strategies, such as passivation techniques or the use of high-quality substrates, are often required, but these may increase fabrication complexity and cost. While the simulations provide idealized values, we recognize that practical fabrication would need to address these challenges to realize the full potential of the optimized design. For each subcell, thickness and BDD have been varied within specific ranges: 0.1 to 1.5 µm for the top and middle cells and 1.5 to 2.5 µm for the bottom cell, with BDD ranging from 1×10^{10} to 1×10^{14} cm−3, across all layers. The results, illustrated in Fig. 3(a-d), demonstrate consistent trends across the three subcells. Each subcell displays its highest V_{OC} when thickness increases and BDD is minimized, due to reduced recombination losses that allow for more effective charge separation. Specifically, the top cell achieves a V_{OC} of 1.27 V, the middle cell 0.793 V, and the bottom cell 0.793 V under optimal conditions, reflecting the positive impact of low defect density and adequate thickness on V_{OC} across the tandem structure.

In terms of J_{SC}, all subcells see an increase with greater thickness due to enhanced photon absorption. However, higher defect densities lead to a decrease in J_{SC} as recombination limits effective charge collection. This relationship between thickness, defect density, and J_{SC} remains consistent across the top, middle, and bottom cells, indicating the critical role of minimized BDD in maintaining high current density.

Similarly, FF for each subcell improves at increased thickness and lower BDD. The top cell reaches a peak FF of 84.25%, the middle cell 69.50%, and the bottom cell also 69.50%, as lower defect densities facilitate more efficient charge transport. Since PCE is a function of V_{OC}, J_{SC}, and FF, the PCE values for each subcell follow these same optimization trends. The champion cells achieve efficiencies of 20.20% for the top cell, 16.35% for the middle cell, and 16.35% for the bottom cell. For top, middle and bottom cell, the cumulative impact of thickness and defect on the various PV parameters have been depicted in the Fig. 3(a-l).

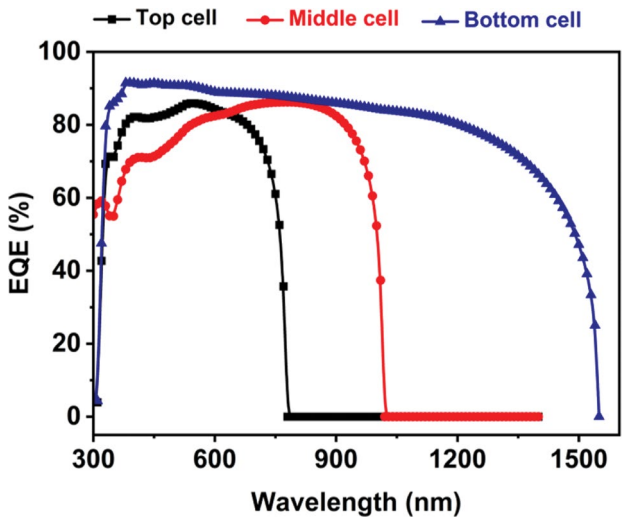

Fig. 2 Obtained EQE curves for the top, middle and bottom subcells

Designing of triple junction tandem solar cell

For the design of the triple junction tandem solar cell (TSC), two filtered spectrums (FS) are calculated to optimize photon absorption and ensure current matching across the subcells. To create three junctions in this work, three subcells have been designed and optimized for their best PV performance. The optimization of all three subcells has been done through various variations in the absorber layer, such as thickness

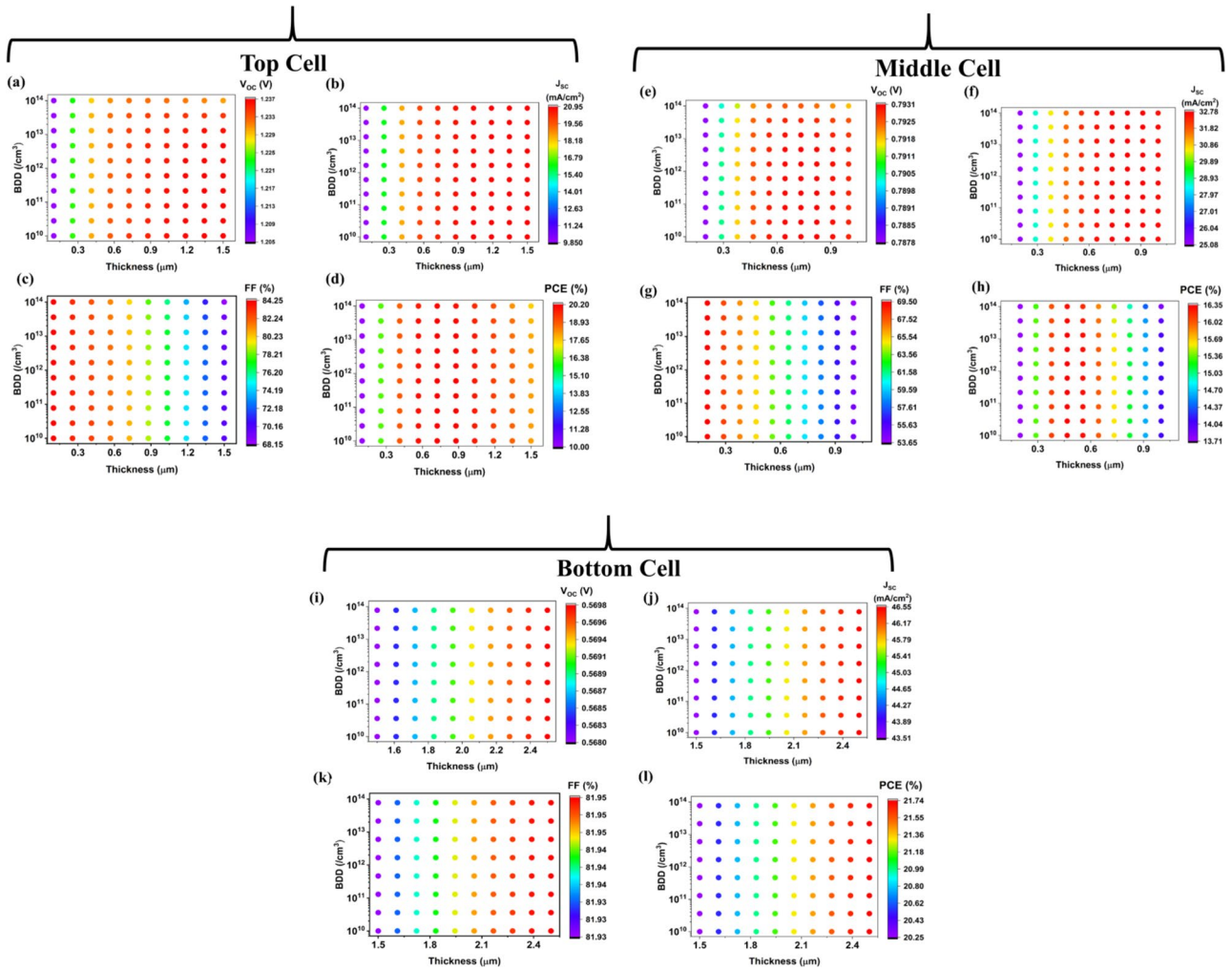

Fig. 3 Cumulative impact of absorber layer thickness and Bulk Defect Density (BDD) on the various photovoltaic (PV) parameters of (**a-d**) the top cell, (**e-h**) the middle cell, and (**i-l**) the bottom cell

and bulk defect density (BDD). It has been observed that the best PV parameters in the top, middle, and bottom cells are achieved at high thickness and low BDD. For the design of the triple-junction tandem configuration, two filtered spectrums (FS1 and FS2) have been calculated to ensure proper current matching in the three subcells. However, it should be noted that the optical limitations of this strategy include assumptions about uniform light distribution and the spectral filtering process, which may not fully account for complex light interactions, such as scattering, reflections, and variations in incident light angle. These factors could introduce deviations in real-world conditions. The first filtered spectrum, FS1, is calculated to assess the illumination that reaches the middle cell after passing through the top cell layers, as shown in Fig. 4(a). The second filtered spectrum, FS2, is calculated to represent the illumination of the bottom cell after light passes through both the top and middle cells, as illustrated in Fig. 4(b). To determine FS1, photons with decreasing intensity are considered as they pass through the absorbing layers of the top cell. This decay in intensity follows an exponential trend, which is quantified using the standard absorption formula shown below. The FS1 calculations are conducted over varying thicknesses of the top cell's absorber layer, ranging from 100 to 1000 nm. With FS1 established, current matching is then achieved between the top and middle subcells by adjusting the thickness and other relevant parameters of the top cell. Through this process, ten matching points are identified, establishing optimal conditions for efficient energy transfer between the top and middle cells. Following the optimization of FS1, FS2 is calculated using the same standard absorption formula (SAF) method, as depicted in Fig. 4(c). FS2 quantifies the light spectrum that reaches the bottom cell after passing through both the top and middle cells, and is calculated across different thickness values of the bottom cell, from 50 to 2000 nm. Once FS2 is established, current matching is re-evaluated across the top, middle, and bottom cells as depicted in the Fig. 4(d). This iterative process identifies

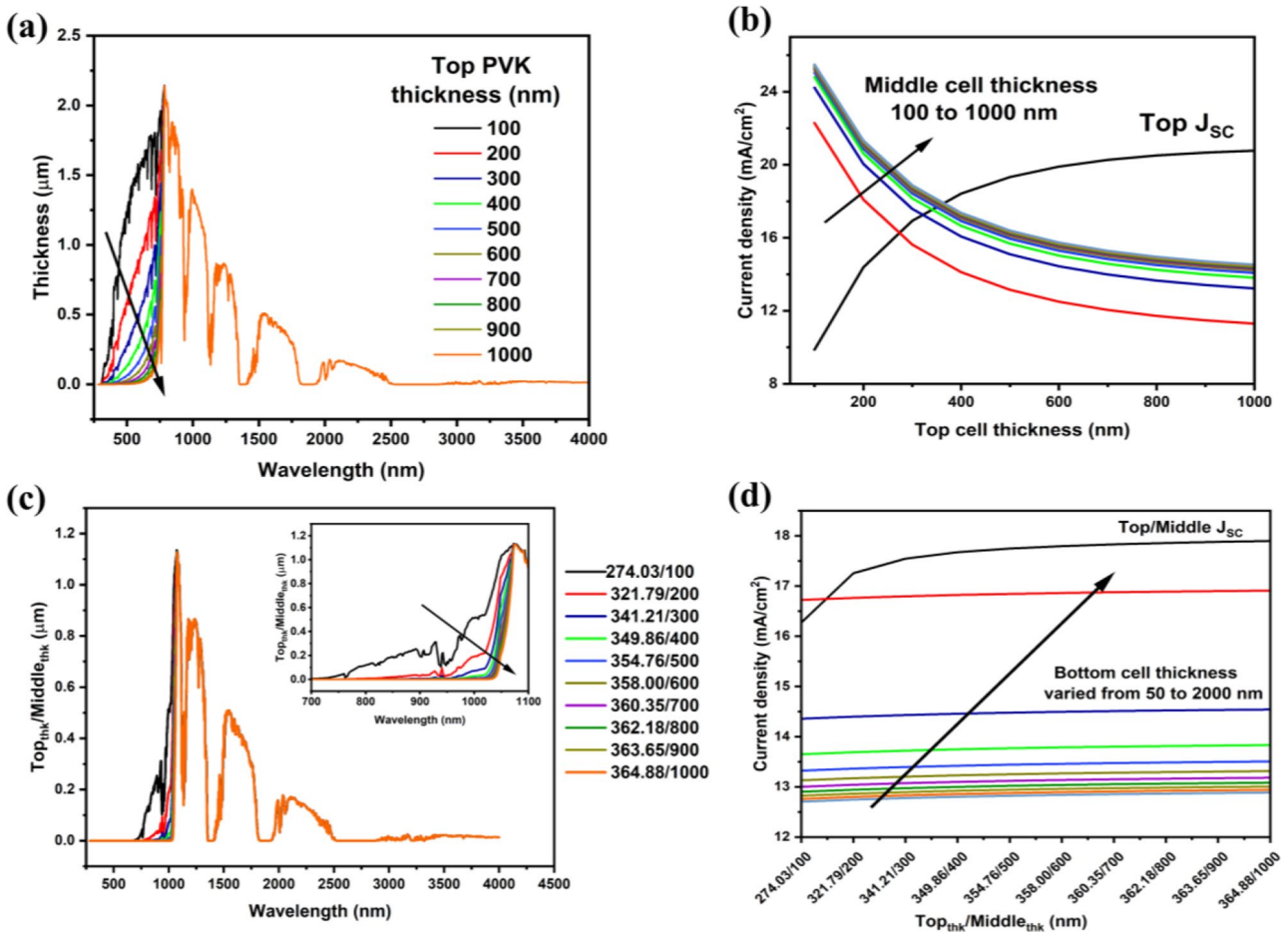

Fig. 4 (**a**) Filtered spectrum calculated by top cell (**b**) Current matching points between top and middle (**c**) Filtered spectrum calculated by both top and middle cell (**d**) current matching points between top, middle and bottom cell

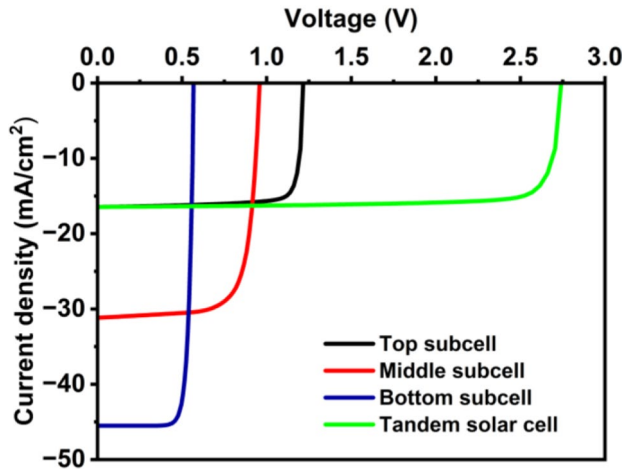

Fig. 5 Obtained JV curves for top, middle, bottom subcell and tripple junction tandem solar cells

one optimal current matching point, where the tandem JV curve for the entire triple-junction TSC is generated. The approach to calculating FS1 and FS2 and achieving current matching is crucial in ensuring that each subcell contributes optimally to the overall power conversion efficiency. By carefully tuning the thicknesses of each subcell and matching the photocurrents, the design maximizes photon utilization and minimizes recombination losses, resulting in a highly efficient triple-junction TSC structure [34, 35].

After achieving current matching points among the top, middle, and bottom cells, the JV (current-voltage) curves for each individual subcell—top, middle, and bottom—as well as for the entire triple-junction tandem solar cell are plotted and provided in Figure (X). These JV curves illustrate the electrical performance characteristics of each cell under optimized conditions, highlighting the impact of thickness and defect density adjustments on their overall photovoltaic (PV) parameters. In Fig. 5, the J-V curves for the top, middle, and bottom subcells were obtained from simulations. The tandem J-V curve was then constructed using the theory of tandem solar cells, where the V_{OC} of the

individual subcells were summed. During the scripting process, it was ensured that the J_{SC} of the tandem cell matched that of the top subcell, as the cells are connected in series. The developed 3JTSC has very promising PV characteristics. Specifically, it achieves high open-circuit voltage (V_{OC}), short-circuit current density (J_{SC}), fill factor (FF), and power conversion efficiency (PCE), indicating efficient photon absorption and charge carrier collection throughout the tandem structure. The V_{OC} reflects the cumulative voltage contribution of each subcell, resulting in a higher total voltage for the tandem design. The J_{SC} demonstrates efficient current matching between subcells, guaranteeing that no one layer restricts current flow, which is crucial for optimal energy conversion. A substantial FF indicates low resistive losses and efficient charge transmission within each layer. These optimised PV parameters demonstrate the tandem design's ability in capturing a wide range of the solar spectrum, with each subcell absorbing differing amounts of light. This design technique outperforms single-junction cells in terms of energy conversion because the triple-junction structure reduces recombination losses while increasing photon utilisation. As a result, this triple-junction tandem solar cell architecture has tremendous potential for high-efficiency solar energy applications, showcasing advances in multi-junction cell engineering.

This includes the integration of novel materials, such as perovskite alloys, 2D materials, or tandem cells incorporating emerging semiconductors, to further enhance the efficiency and stability of tandem solar cells. Additionally, the research highlights the challenges and opportunities associated with scaling up these technologies, including considerations related to material availability, large-scale manufacturing processes, and cost reduction strategies necessary for commercial viability. These insights offer valuable guidance for the next steps in advancing tandem solar cell technologies.

Conclusion

In this work, the optimization of a 3JTSC have been done, which includes customised thicknesses and low defect concentrations for each subcell, has resulted in significant gains in photovoltaic efficiency. This design maximises light absorption and charge collection by computing filtered spectrums (FS1 and FS2) and matching current across the top, middle, and bottom subcells. The JV curves for each subcell and the entire tandem configuration reveal high V_{OC}- 2.705 V, J_{SC}- 16.45 mA/cm^2, FF- 83.40%, and PCE- 37.74%, collectively showcasing the advantages of the multi-junction approach. The champion 3JTSC design takes advantage of each subcell's unique spectral absorption characteristics, allowing for more effective solar spectrum utilisation and lower recombination losses. This study demonstrates that multi-junction tandem solar cells can greatly outperform single-junction devices, making them a feasible path for obtaining high-efficiency solar energy solutions. The findings emphasise the importance of structural and spectral tailoring in tandem cell design, opening the door for future advances in high-performance solar cell technology.

Data availability Data will be made available upon request from the corresponding authors.

Declarations

Competing interests The authors declare that they have no known competing financial interests.

References

1. Lee, T.D., Ebong, A.U.: A review of thin film solar cell technologies and challenges. Renew. Sustain. Energy Rev. **70**, 1286–1297 (2017)
2. Adachi, S.: Optical Constants of Crystalline and Amorphous Semiconductors: Numerical data and Graphical Information. Springer Science & Business Media (2013)
3. Shrivastav, N., Madan, J., Pandey, R.: Maximizing performance in $Cs_2CuBiCl_6$ perovskite cells through machine learning-driven absorber layer parameter analysis. Mater. Lett. **359**, 135929 (2024)
4. Kim, J.Y., et al.: Efficient tandem polymer solar cells fabricated by all-solution processing. Science. **317**(5835), 222–225 (2007)
5. Shrivastav, N., Madan, J., Pandey, R.: Optimizing tandem solar cells efficiency through current matching technique in lead-free perovskite/c-Si and lead-free perovskite/CIGS absorbers. Indian J. Phys. 1–9, (2024)
6. Adewoyin, A.D., Olopade, M.A., Oyebola, O.O., Chendo, M.A.: Development of CZTGS/CZTS tandem thin film solar cell using SCAPS-1D. Optik. **176**, 132–142 (2019)
7. Shrivastav, N., Madan, J., Hossain, M.K., Albaqami, M.D., Pandey, R.: Design and simulation of three-junction all perovskite tandem solar cells: A path to enhanced photovoltaic performance. Mater. Lett. **362**, 136169 (2024)
8. Abdelkadir, A.A., Oublal, E., Sahal, M.: Theoretical analyses of new tandem solar cells based on CdTe using SCAPS-1D, in AIP Conference Proceedings, vol. 2761, no. 1: AIP Publishing. (2023)

9. Wali, Q., Elumalai, N.K., Iqbal, Y., Uddin, A., Jose, R.: Tandem perovskite solar cells. Renew. Sustain. Energy Rev. **84**, 89–110 (2018)
10. Li, H., Zhang, W.: Perovskite tandem solar cells: from fundamentals to commercial deployment, Chemical Reviews, vol. 120, no. 18, pp. 9835–9950, (2020)
11. Jafarzadeh, F., Aghili, H., Nikbakht, H., Javadpour, S.: Design and optimization of highly efficient perovskite/homojunction SnS tandem solar cells using SCAPS-1D, Solar Energy, **236**, 195–205 (2022)
12. Kumar, A., Singh, S., Mohammed, M.K., Shalan, A.E.: Computational modelling of two terminal CIGS/perovskite tandem solar cells with power conversion efficiency of 23.1%, European journal of inorganic chemistry, vol. no. 47, pp. 4959–4969, 2021. (2021)
13. Duha, A.U., Borunda, M.F.: Optimization of a Pb-free all-perovskite tandem solar cell with 30.85% efficiency. Opt. Mater. **123**, 111891 (2022)
14. Duan, L., et al.: Stability challenges for the commercialization of perovskite–silicon tandem solar cells. Nat. Reviews Mater. **8**(4), 261–281 (2023)
15. Fan, Q., et al.: Lead-free halide perovskite nanocrystals: Crystal structures, synthesis, stabilities, and optical properties. Angew. Chem. Int. Ed. **59**(3), 1030–1046 (2020)
16. Miao, S., et al.: 2D Material and Perovskite Heterostructure for Optoelectronic Applications, Nanomaterials, vol. 12, no. 12, p. 2100, (2022)
17. Liu, M., Johnston, M.B., Snaith, H.J.: Efficient planar heterojunction perovskite solar cells by vapour deposition. Nature. **501**(7467), 395–398 (2013)
18. Papež, N., et al.: Performance analysis of GaAs based solar cells under gamma irradiation. Appl. Surf. Sci. **510**, 145329 (2020)
19. Green, M., Dunlop, E., Hohl-Ebinger, J., Yoshita, M., Kopidakis, N., Hao, X.: Solar cell efficiency tables (version 57), Progress in photovoltaics: research and applications. **29**(1), 3–15 (2021)
20. Zheng, J., et al.: Monolithic perovskite–perovskite–silicon triple-junction tandem solar cell with an efficiency of over 20%. ACS Energy Lett. **7**(9), 3003–3005 (2022)
21. Fan, K., Li, R., Chen, J., Shi, W., Peng, T.: Recent development of dye-sensitized solar cells based on flexible substrates. Sci. Adv. Mater. **5**(11), 1596–1626 (2013)
22. Shrivastav, N., Madan, J., Pandey, R.: Advancing accuracy in Perovskite Tandem Solar cell efficiency via transfer matrix-based realistic device simulations. J. Electron. Mater. 1–10 (2024)
23. Aliaghayee, M.: Optimization of the perovskite solar cell design with layer thickness engineering for improving the photovoltaic response using SCAPS-1D. J. Electron. Mater. **52**(4), 2475–2491 (2023)
24. Islam, M.T., et al.: Investigation of CsSn 0.5 Ge 0.5 I 3-on-Si tandem solar device utilizing SCAPS simulation. IEEE Trans. Electron. Devices. **68**(2), 618–625 (2021)
25. Kumar, A., Chitkara, M., Dhillon, G.: Effect of gadolinium substitution on structural, morphological, and electrical properties of SnO2 thin films. J. Mater. Sci.: Mater. Electron. **34**(4), 319 (2023)
26. Yu, Z., et al.: Simplified interconnection structure based on C60/SnO2-x for all-perovskite tandem solar cells. Nat. Energy. **5**(9), 657–665 (2020)
27. Rassol, R.A., Hasan, R.F., Ahmed, S.M.: Numerical Analysis of SnO2/Zn2SnO4/n-CdS/p-CdTe solar cell using the SCAPS-1D Simulation Software. Iraqi J. Sci. 505–516 (2021)
28. Xiao, K., et al.: Solution-processed monolithic all-perovskite triple-junction solar cells with efficiency exceeding 20%. ACS Energy Lett. **5**(9), 2819–2826 (2020)
29. McMeekin, D.P., et al.: Solution-processed all-perovskite multi-junction solar cells, Joule, vol. 3, no. 2, pp. 387–401, (2019)
30. Thakur, A., Singh, D., Gill, S.K.: Numerical simulations of 26.11% efficient planar CH3NH3PbI3 perovskite nip solar cell. Mater. Today: Proc. **71**, 195–201 (2022)
31. Dogra, A.R., Kumar, P., Sharma, V., Malik, P., Khanra, P., Kapoor, M.: Deposition of nanoparticles layer on ITO substrate and its application for alignment control of liquid crystal, in AIP Conference Proceedings, vol. 2357, no. 1: AIP Publishing LLC, p. 050019. (2022)
32. Wang, J., et al.: Tandem organic solar cells with 20.6% efficiency enabled by reduced voltage losses. Natl. Sci. Rev. **10**(6), nwad085 (2023)
33. Chin, X.Y., et al.: Interface passivation for 31.25%-efficient perovskite/silicon tandem solar cells, Science, vol. 381, no. 6653, pp. 59–63, (2023)
34. Zheng, X., Alsalloum, A.Y., Hou, Y., Sargent, E.H., Bakr, O.M.: All-perovskite tandem solar cells: A roadmap to uniting high efficiency with high stability. Acc. Mater. Res. **1**(1), 63–76 (2020)
35. Jost, M., et al.: Perovskite/CIGS tandem solar cells: From certified 24.2% toward 30% and beyond, ACS energy letters, **7**(4), 1298–1307 (2022)
36. Nogay, G., et al.: 25.1%-efficient monolithic perovskite/silicon tandem solar cell based on ap-type monocrystalline textured silicon wafer and high-temperature passivating contacts. ACS Energy Lett. **4**(4), 844–845 (2019)
37. Park, I.J., Park, J.H., Ji, S.G., Park, M.-A., Jang, J.H., Kim, J.Y.: A three-terminal monolithic perovskite/Si tandem solar cell characterization platform. Joule. **3**(3), 807–818 (2019)